

Published in final edited form as:

Neurosci Biobehav Rev. 2004 September ; 28(5): 449–461. doi:10.1016/j.neubiorev.2004.06.007.

Mapping brain function in freely moving subjects

Daniel P. Holschneider^{a,b,*} and Jean-Michel I. Maarek^c

^aDepartments of Psychiatry and the Behavioral Sciences, Neurology, Cell and Neurobiology, University of Southern California, 1333 San Pablo St., BMT 401, MC 9112, Los Angeles, CA 90089-9112, USA

^bVA Greater Los Angeles Healthcare System, Los Angeles, CA 90073, USA

^cDepartment of Biomedical Engineering, University of Southern California, 3650 S. McClintock, Los Angeles, CA 90089-1451, USA

Abstract

Expression of many fundamental mammalian behaviors such as, for example, aggression, mating, foraging or social behaviors, depend on locomotor activity. A central dilemma in the functional neuroimaging of these behaviors has been the fact that conventional neuroimaging techniques generally rely on immobilization of the subject, which extinguishes all but the simplest activity. Ideally, imaging could occur in freely moving subjects, while presenting minimal interference with the subject's natural behavior. Here we provide an overview of several approaches that have been undertaken in the past to achieve this aim in both tethered and freely moving animals, as well as in nonrestrained human subjects. Applications of specific radiotracers to single photon emission computed tomography and positron emission tomography are discussed in which brain activation is imaged after completion of the behavioral task and capture of the tracer. Potential applications to clinical neuropsychiatry are discussed, as well as challenges inherent to constraint-free functional neuroimaging. Future applications of these methods promise to increase our understanding of the neural circuits underlying mammalian behavior in health and disease.

Keywords

Brain mapping; Nontethered; Freely moving; Positron emission tomography; Single photon emission computed tomography; Behavior; Tc^{99m}-HMPAO; Tc^{99m}-bicisate; Cu⁶⁴-PTSM

1. Introduction

Functional neuroimaging represents an essential technology toward understanding the complex relationship between behavior and underlying brain function. A central dilemma, however, in conventional neuroimaging protocols is that immobilization of the subject, necessary to avoid movement artifact, extinguishes all but the simplest behaviors. The result is that brain function remains poorly understood of such core mammalian behaviors as, for

example, aggression, mating, foraging, and social interaction—all behaviors dependent on freedom of movement.

In human subjects, the need to largely immobilize subjects during imaging has restricted its application to paradigms that can be performed readily within the scanner. Usually these have involved presentation of sensory stimuli or cognitive tasks presented from a computer screen. However, the situation of the subject's exposure while supine inside the scanner may not be transferable to an unencumbered, natural experience. Reconstruction of a mental state, for instance, during presentation of an emotionally laden photograph is likely to be partial, at best. Motor tasks, when undertaken, have been simple (e.g. finger tapping, ankle flexion and extension) so that immobilization of the subject's head can be maintained.

In animal studies the problem is similar. Immobilization in awake animals during imaging limits the behaviors that can be examined, and introduces the additional variables of restraint stress which can alter the scan, for example, through resultant acid–base imbalances [1] or through muscle artifact [2]. Acclimation of animals to physical restraint is partial at best. For example, biochemical studies measuring norepinephrine, epinephrine, and corticosterone levels have indicated that it may be difficult to adapt rats to daily episodes of immobilization stress, even after 2 weeks of daily exposure [3,4]. Furthermore, the use of even low doses of an anesthetic or neurosedative agents for stress relief in animals inside the scanner may confound meaningful interpretation of the results [5–9]. Ideally, functional neuroimaging of mammalian behaviors could occur in freely moving subjects, while presenting minimal interference with the subject's natural behavior. This review provides a brief overview of different approaches that have been undertaken in the past to begin to achieve this aim in tethered and freely moving animals, as well as in unrestrained human subjects. Applications of specific radiotracers to single photon emission computed tomography (SPECT) and positron emission tomography (PET) are described in which brain activation is imaged after completion of the behavioral task and capture of the tracer. Potential applications to clinical neuropsychiatry are discussed, as well as challenges inherent to constraint-free functional neuroimaging.

2. Past studies

2.1. Studies during partial immobilization

A large number of studies have examined functional brain activation in partially immobilized subjects. Generally such studies involve free movement of a limb, while the subject's head remains immobilized to avoid motion artifact during brain imaging. Thus, for instance, brain activation in human subjects has been studied with SPECT during supine exercise [10,11] and cycling [12], in which the head remained immobilized inside the scanner. Likewise, PET has been applied to the brain imaging of manual tool use in monkeys, while these animals have their head and torso restrained in a chair [13], and other similar examples could be cited. While many such paradigms may be appropriate for the study of the neural circuitry underlying isolated limb movement, their application to complex behaviors and emotional processes is restricted by the physical constraints and stress of the scanner environment.

2.2. Studies in tethered animals

Several research groups have described the measurement of regional cerebral blood flow (rCBF) in ambulatory animals by injection of radiotracers [14] or radiolabeled microspheres [15–18] through catheters, attached via an implanted body port to an external swivel arm and motor-driven infusion pump. Also applied to the measurement of CBF in ambulatory, tethered animals has been the hydrogen-gas clearance method, in which hydrogen wash-out curves are calculated after H₂-gas is applied by inhalation [19,20]. The extent to which tethering reshapes ‘normal’ behavior in these paradigms is likely substantial. Though, perhaps less stressful than direct handling of the animal [21], tethering results in abnormal responses including decreased exploratory activity, increased stereotypies, aggression and immobility, as well as an altered stress hormone response [22–26]. Furthermore, tethering is practical only in the study of behaviors of animals in isolation and is limited to a subset of behaviors, which present a low risk of entanglement of the animal with its cable. Thus, for instance, behaviors such as social encounters, mating and aggression are difficult to study in tethered subjects.

Other techniques requiring tethers, as well as head-mounted imaging probes include the assessment of local changes in brain perfusion by transcranial Doppler ultrasound [27], or the assessment of neuronal activity in living tissues using optical dyes by optical imaging two-photon microscopy [28]. These techniques provide a detailed assessment of regional changes in brain function. However, only a limited number of regions in surface areas of the brain can be examined. Artifacts due to motion of the brain relative to the skull have also presented challenges here for the spatial resolution using optical imaging.

2.3. Studies in freely moving animals

Several investigators have reported functional brain activation in nontethered, freely moving animals. Brain electrical recordings using radiotelemetry offer the advantage of detailed information regarding the temporal and spatial synchronization of mental processes, however, only limited cortical and subcortical areas can be mapped electrophysiologically in a single subject [29–34]. Brain functional activation in animals has also been explored using measurement of the early response genes [35,36]. Early response genes, such as *c-fos*, are rapidly induced in response to a variety of extracellular stimuli. Assessment of *c-fos* mRNA or protein levels can then be used as markers of cellular activation. In such studies, animals have been exposed, for instance, to an acoustic challenge [37] and changes in the early gene response have been subsequently assessed using autoradiographic detection of changes in the expression of the *c-fos* gene. Unlike brain electrical recording, the *c-fos* technique offers the possibility of comprehensive brain maps in cortical, as well as subcortical regions. However, in order to elicit robust *c-fos* expression, a continuous single exposure or intermittent, repeated exposure to the stimulus is required, typically for extended cumulative periods of 0.5–3 h. Indeed, most studies have required prolonged direct electrical brain stimulation, rather than behavioral activation, to elicit changes in the early gene response. Furthermore, discrepancies between the distribution of *c-fos* and metabolic studies using 2-deoxyglucose uptake have been reported, and it is now believed that *c-fos* may be a good marker of long term functional changes in neurons (or subpopulations of neurons), rather than acute increases in neuronal activity [38].

Another histologic approach to visualizing long-term functional changes in neurons with resolution at the cellular and subcellular level is the assessment of cytochrome oxidase activity. Cytochrome oxidase (CO) is a mitochondrial enzyme, which is rate-limiting for oxidative energy metabolism of ATP. Because the metabolic capacity of neurons is determined by their ability to use ATP for the high energy-requiring membrane potentials involved in synaptic transmission, a sustained increase in the energy demand of the cell requires increased production of the CO enzyme [39]. Assessment of CO enzymatic activity in the brain has mainly been used to investigate relatively large metabolic changes in neuronal activity such as those elicited after eye enucleation [40,41], disruption of blood circulation or hypoxia [42,43], ageing [44], and electroconvulsive treatment [45], though more subtle applications to learning [46–48] and chronic exercise [49] have also been undertaken. Unlike other types of metabolic mapping such as 2-deoxyglucose, whose uptake is determined by neuronal activity during experimental periods of 25–45 min, CO mapping reveals neuronal activity as it occurs over long periods (hours to weeks), with changes that persist after cessation of the specific behavior. This may be advantageous if one wishes to study average brain activity throughout the full cycle of normal daily activities. Thus, for instance, rats exposed to 6 months of regular exercise demonstrated selected increases in neuronal activity in motor cortex (18%) and dorsolateral caudate-putamen (17%), despite the fact that they engaged also in other non-exercise related behaviors during this time [49]. Rats exposed to classical conditioning in an auditory paradigm showed increases in CO activity at upper auditory structures (medial geniculate nucleus and secondary auditory cortices), despite the fact that training occurred over several days, and was interspersed with a number of routine animal behaviors during this time period [47].

2.4. Constraint-free brain mapping studies using radiolabeled 2-deoxyglucose

The problem of behavioral restraint can be solved if radiotracers are administered by non-agitating means, and regional brain activation is imaged after completion of the behavioral task and capture of the tracer. One method, which lends itself to this, is the quantitative measurement of glucose metabolism. Glucose is the primary fuel for the central nervous system. Since glucose itself is metabolized too rapidly for adequate study, use of radiolabeled glucose analogues, e.g. [^{14}C]-2-deoxyglucose ([^{14}C]-2-DG) [50] or [^{18}F]-fluoro-2-deoxyglucose ([^{18}F]-FDG) [51], allow measurement of brain metabolism. 2-Deoxyglucose (2-DG) crosses the blood–brain barrier and is phosphorylated by the hexokinase system to DG-6-phosphate, similarly to glucose. However, in contrast to glucose-6-phosphate, which further metabolizes to carbon dioxide and water, DG-6-phosphate remains trapped in the tissue for an extended period of time. This unique metabolic behavior allows radiolabeled 2-DG to be used as a proxy to track glucose utilization. Since imaging of brain metabolism typically takes place after tracer uptake is complete and relatively imperturbable, this method is suitable for neuroimaging in nontethered, ambulatory subjects. Using PET, this approach has been applied to functional brain mapping in human subjects during treadmill walking, in which ^{18}F -FDG was administered intravenously during exercise, and imaging was performed 40 min thereafter [52, 53]. Similar PET studies have been applied to the mapping of visual recognition memory in the behaving baboon [54]. Using autoradiography and radiolabeled 2-DG brain function has been mapped also in rats during performance of the Morris Water Maze [55].

during drinking behavior [56], during a forelimb grasping task [57], during treadmill walking [58], during self-administration of phencyclidine [59], metamphetamine [60] or ethanol [61], as well as during the two stages of the activity-rest cycle [62].

The primary drawback of radiolabeled 2-DG is that the duration of the uptake and capture of the tracer is around 25–45 min [63], which is suboptimal given the fact that many behaviors are more short-lived. In principle, delivery of a radiotracer that reaches a cerebral equilibrium in a shorter time frame than 2-DG, would allow imaging of behaviors with a greater temporal resolution. Tracers with the shortest half-lives, however, may not necessarily be the most suitable for capturing brain activation in freely moving subjects. For instance, H_2^{15}O , the classic cerebral blood flow tracer for PET studies, while providing excellent temporal resolution for the capture of short-lived behaviors, is not suitable because its brief radioactive half-life ($t_{1/2} = 2.05$ min) allows insufficient time for tracer injection in the freely moving subject, followed by positioning of the subject and completion of a scan. Furthermore, because it is a diffusible tracer, the distribution of H_2^{15}O would continue to change in response to any manipulation of the experimental subject, even after the behavioral exposure. Even the half-life of a tracer such as ^{13}N -ammonia ($t_{1/2} = 10.0$ min), which undergoes intracellular metabolic trapping as ^{13}N -glutamine, may not allow a sufficient time frame [64]. In animals, injection of micro-spheres labeled with a short-lived generator-produced positron emitter like Ga^{68} ($t_{1/2} = 67.6$ min) might be feasible, but would require arterial infusion [65,66].

3. Alternative radiotracers for constraint-free brain mapping with improved temporal resolution

The ideal tracer for constraint-free functional neuroimaging would have the following properties: (a) in vitro chemical stability prior to administration, (b) nontoxic and suitable for injection, (c) a high lipid solubility or substrate of a blood barrier transporter (e.g. glucose), with ready passage of the tracer across the blood–brain barrier, (d) a high extraction by the brain, with microsphere-like retention after a single passage, with a distribution in the brain that is proportional to rCBF. This is important since extractable tracers, compared to diffusible tracers, do not directly measure of rCBF but rather are surrogate measures of perfusion, (e) a prolonged retention in brain tissue with a fixed distribution that is independent of rCBF variations occurring after the fixation time, (f) inability of radiolabeled metabolites to cross the blood–brain barrier and/or rapid clearance of these metabolites from blood, (g) a trapping mechanism which is unaltered in pathology, (h) a radioactive half-life sufficiently long to allow time for administration of the tracer during occurrence of the behavior and subsequent positioning of the subject inside the scanner for data acquisition, (i) a radioactive half-life sufficiently short to allow decay within a few hours to days to minimize radiation exposure, and allow for rescanning of the subject as his own control, (j) a photon energy compatible with currently used instrumentation.

3.1. SPECT

For functional neuroimaging using SPECT, several tracers have been used that meet several of the above-mentioned requirements. Technetium-99m-hexamethyl-proyleneamine oxime ($\text{Tc}^{99\text{m}}\text{-D,L-HMPAO}$ or exametazime; CeretecTM, radioactive $t_{1/2} = 6.03$ h, Nycomed-Amersham, Little Chalfont, UK), a commercially available tracer, has been used to study brain activation in freely-moving human subjects during walking [67], during cycling on a stationary bicycle [68], and in nonrestrained subjects during performance of the Wisconsin Card Sorting Test [69]. The $^{99\text{m}}\text{Tc}$ complex of HMPAO (but not HMPAO itself) readily passes the intact blood–brain barrier, and brain uptake of $\text{Tc}^{99\text{m}}\text{-D,L-HMPAO}$ closely reflects regional CBF [70]. Brain uptake is around 2–3% of the injected dose and is reached within 1 min after injection. The single-pass extraction is about 70–80% with normal blood flows of 50 ml/100 g/min. Thereafter, the tracer is retained in brain tissue, probably due to intracellular conversion of reduced glutathione, converting it to a meso isomer that is trapped inside the brain. In rats, evidence suggests there may also be conversion to a hydrophilic product, $^{99\text{m}}\text{Tc}$ -pertechnetate, and binding to intracellular components. Up to 15% of the cerebral activity washes out of the brain within 15 min post injection. This initial backdiffusion is more prominent in high blood flow regions, and explains why $\text{Tc}^{99\text{m}}\text{-D,L-HMPAO}$ tends to slightly underestimate higher regional CBF [71,72]. After this initial backdiffusion of the tracer from brain to blood, there is little loss of activity for the following 24 h, except by physical decay of the isotope. This stability of distribution within the brain is essential during image acquisition, and is one reason why earlier perfusion agents such as ^{123}I -labeled iodoamphetamine (IMP, Spectamine, Medi-Physics, Inc., Emeryville, CA) have fallen into disuse. IMP, while demonstrating a high first-pass extraction fraction (85–95%), shows substantial washout and redistribution, such that perfusion patterns at an hour post-administration no longer represent perfusion at the time of injection [73–76]. By comparison, imaging with HMPAO can take place from 2 min to 4 h post injection. In the past, the major problem with HMPAO had been the instability of this agent in vitro after reconstitution, requiring that it be injected less than 30 min after preparation. Stabilized forms of $\text{Tc}^{99\text{m}}\text{-D,L-HMPAO}$ using either methylene blue or cobalt chloride have recently become available, and can extend stability to 4–6 h [77]. However, blood clearance of labeled metabolites is not rapid, limiting the dosimetry in humans. Consequently, other agents using $\text{Tc}^{99\text{m}}$ complexes have been explored as alternate cerebral blood flow tracers.

One such agent is ethylcysteinate dimer [$\text{Tc}^{99\text{m}}\text{-L,L-ECD}$] bicesate, which has been commercially available ($\text{Tc}^{99\text{m}}\text{-ECD}$, Neurolite, Dupont-Pharma, Stevenage, UK). ECD has been applied to functional neuroimaging paradigms in which administration of the tracer occurs outside of the scanner environment. In these studies, subjects were seated at a table, and were presented with a spatial working memory task [78], a verbal fluency task [79], or a Stroop interference task [80] following administration of ECD, and prior to scanning. ECD has in vitro stability up to at least 4 h; it is a small lipophilic molecule without significant protein binding that rapidly crosses the blood–brain barrier, reaching its maximum within 5 min (4–7% uptake of the injected dose in brain). There is a 70% first-pass extraction in brain. Intracellular retention of the radioactive material is thought to be caused by enzymatic trapping when the L-diester is hydrolyzed to a polar monoacid–monoester complex [81,82].

These polar metabolites cannot diffuse back through the blood–brain barrier [83]. The distribution of radioactivity for Tc^{99m}-ECD brain SPECT reflects that of blood flow in most clinical situations; however, regional differences in enzymatic activity may cause regional differences in the retention efficiency of Tc^{99m}-ECD. The occipital lobe has shown relatively high accumulation [84], which may be caused by high enzymatic activity in the area. Kinetic analysis has demonstrated a small amount of back-diffusion of ECD compared with that of HMPAO. Washout is slow and estimated at 6% per hour for the first 6 h. There is no relationship between the back-diffusion rate and rCBF [82]. Imaging can take place from 2 min to 2 h post injection. Elimination of ECD from the blood and lungs is rapid, resulting in less than 5% of the injected dose remaining in the blood by 1-h post administration. The rapid urinary excretion allows administration of higher doses of ECD. ECD images of the head show significantly less background facial uptake and retention when compared to HMPAO images [85]. These factors, together with the higher gray-matter-to-white-matter ratio, contribute to the better image quality obtained with ECD in comparison with HMPAO (gray-matter-to-white-matter ratio 2–3:1 for HMPAO versus 4:1 for ECD) [86]. Differences in the gray-matter-to-white-matter ratios of HMPAO and ECD underscore the differences underlying the chemical reactions required for tissue retention of these tracers, as well as how closely these tracers may approximate true cerebral perfusion, as compared to that measured using H₂¹⁵O PET. Unlike earlier tracers such as the ¹²³I-labeled amines [74,75], neither ECD nor HMPAO redistributes in the brain.

Although both HMPAO and ECD are distributed proportionally to regional CBF, their retention is not completely linear with rCBF because of an initial back-diffusion. High blood flow may be underestimated and low blood flow may be overestimated with both tracers [87,88]. Furthermore, a discrepancy between blood flow and accumulation has been documented during the subacute phase of cerebral infarction. SPECT with Tc^{99m}-ECD (unlike HMPAO) commonly reveals the infarcted region as a hypoactive area, even in the presence of postischemic hyperperfusion. This finding indicates reduced retention efficiency in infarcted brain tissue, which may be attributable to an impaired enzymatic system [89–91]. It is important to realize that all SPECT methods, with the exception of Xe¹³³-SPECT—not mentioned in this review because it requires positioning in the scanner during tracer administration—do not give quantitative information in blood flow units, and are limited to detection of CBF ‘patterns’.

3.2. PET

The gold standard for PET CBF measurements is H₂¹⁵O PET with detection of the arterial input function by arterial blood sampling or imaging of a suitable large artery. However, this methodology does not adapt to constraint-free neuroimaging because it requires a dynamic data acquisition, with the subject inside the scanner at the time of tracer administration. For PET applications there are few currently available commercial tracers that meet the requirements necessary for constraint-free neuroimaging. A tracer which has been proposed as a single-pass flow tracer for PET applications is the copper(II) complex of pyruvaldehyde bis(N⁴-methylthiosemicarbazone), Cu-PTSM [92]. Copper-PTSM, has been used to assess cerebral and myocardial perfusion in humans and animals [92–96], and has been used to map somatosensory brain function in the immobilized baboon [97]. When labeled with ⁶¹Cu

($t_{1/2} = 3.3$ h), ^{64}Cu ($t_{1/2} = 12.7$ h), or ^{67}Cu ($t_{1/2} = 58.5$ h), Cu-PTSM might be appropriate for neuroimaging in freely moving subjects, whereas the shorter lived isotopes of copper (Cu^{60} $t_{1/2} = 23.7$ min, Cu^{62} $t_{1/2} = 9.7$ min) might be more appropriate for imaging in immobilized subjects. These copper labeled complexes show high lipophilicity and are extracted into the brain with a high efficiency (Extraction fraction 0.90–0.76 for cerebral blood flows of 36–89 ml/min/100 g) [92,96,98]. While this extraction rate is lower than that of [^{123}I]-*N*-isopropyl-*p*-iodo-amphetamine (IMP), it is higher than the metal-labeled SPECT radiopharmaceuticals that have been proposed as cerebral blood flow agents (e.g. $^{99\text{m}}\text{Tc}$ -HMPAO, -ECD) [72,99]. Correlation in rats between regional uptake of copper and relative regional CBF measured by [^{125}I]-iodoantipyrine shows a good correlation ($r = 0.98$) [95]. Data suggests a microsphere-like retention of Cu-PTSM, with absence of washout and a clearance half-life in brain of 140 min. The retention mechanism of Cu-PTSM is reported to rely on the irreversible binding of copper to intracellular thiols (predominantly glutathione/metallothionein), with a concomitant reduction of copper (II) to copper (I) [100]. After ~1 min, all of the radioactivity in blood is due to metabolites, and these do not penetrate the blood–brain barrier [92]. PET images obtained in baboon brain with the use of ^{64}Cu -PTSM and H_2^{15}O are qualitatively and quantitatively very similar, despite the different principles underlying the imaging of CBF with these tracers, with gray to white matter uptake ratios of 2.67 for Cu-PTSM and 2.42 for H_2^{15}O [92]. No redistribution of ^{64}Cu is observed in baboon brain during 2 h of imaging [92]. Presence in some species of the binding of ^{62}Cu -PTSM to albumin has been reported [101], resulting in a correction factor being necessary for assessment of the arterial input function needed for accurate quantification of regional CBF [102]. However, for nonquantitative studies, such as would typically be most practical for constraint-free imaging, the relative distribution of Cu-PTSM correlates well with regional CBF obtained by ^{15}O -water PET [96]. Recent work from our laboratory has used ^{64}Cu -PTSM to map functional brain activation during treadmill walking in rats (Fig. 1).

4. Mode of administration of the radiotracer

A critical issue to the success of imaging in freely moving subjects is the mode of administration of the radiotracer. Ideally administration would occur with minimal interference with the subject's natural behavior. This is the case, not only because the physical act of injection may itself terminate the behavior, but also because it is well known that stress associated with an injection may substantially modify a subject's behavior. In animals, even minor routine handling procedures can induce a marked stress, although the animal has been trained to this procedure and looks quiet [21]. Furthermore, it has been suggested that the mode of administration of a drug—either by manual injection or self-administration—may result in different effects on brain metabolism [59].

One low-stress approach to administration of radiotracers in monkeys has been to train them to self-administer an oral dose of ^{18}F -FDG prior to a behavioral challenge, followed thereafter by anesthesia and PET scanning [103]. Oral administration studies, however, are complicated by the problem of delayed, often unpredictable, absorption of the radiotracer from the gastrointestinal tract. Such delayed absorption results in a prolonged and poorly defined temporal 'window' for capturing behavioral brain activation during which neuronal

uptake of the radiotracer is most active. In addition, training animal subjects to predictably self-administer the entire aliquot of the oral radiotracer suspension and not spit out all or parts of the solution, presents a substantial challenge [103].

A device which would allow radiotracer administration by remote control would solve the problem of behavioral restraint confounding measures of brain metabolism or blood flow, and should have applications for functional neuroimaging in freely-moving subjects. In principle, a portable pump, implanted or worn outside the body, could be used to administer the tracer. Programmable, portable infusion pumps with weights as low as 65 g are commercially available [104]. However, none of these infusion devices offer rates of drug delivery above approximately 10 $\mu\text{l/s}$, which may make delivery of a discrete bolus of a radiotracer difficult. For veterinary applications, the Pegasus[®] pump (Instech Laboratories, Inc., Plymouth Meeting, PA), a pump worn externally in a vest, offers programmability and remote activation at a maximum infusion rate of 28 $\mu\text{l/s}$. Its weight, at 180 g, makes it appropriate for use in animals weighing greater than ~ 2 kg. However, for brain mapping studies in small species (e.g. rats, mice), no commercial device currently exists which offers the portability, minimal invasiveness, high flow rates and remote activation needed to facilitate constraint-free imaging. Small, implantable, slow-release, osmotic pumps, elastomeric pumps or vapor pressure pumps are commercially available, however, allow only examination of chronic drug effects (days to weeks) and cannot be used for purposes of functional neuroimaging. Furthermore, these pumps do not have the ability to be controlled by remote activation.

To address the problem of immobilization and tethering, as well as the need for rapid assessment in neuroimaging studies in small animals, we have recently developed a self-contained, fully implantable miniature infusion pump that allows injection by remote activation of a bolus radiotracer at an average flow rate of ~ 140 $\mu\text{l/s}$ [105]. Use of this pump has been validated as a tool for functional neuroimaging in rats in three separate behavioral tasks: treadmill walking, auditory perception and acute footshock [106–108]. In these studies, we used the cerebral perfusion tracer [¹⁴C]-iodoantipyrine, which unlike the previously discussed extraction tracers, is diffusible. In order to avoid nonspecific diffusion, rapid euthanasia is required, with rapid removal and flash freezing of the brain in preparation for autoradiographic analysis of the regional distribution of tissue radioactivity. Our mapping studies have demonstrated the following points: (a) The pump allows the capture of ‘snapshots’ of cerebral activity, with an estimated temporal resolution of ~ 10 s, while autoradiographic analysis of the images offers a spatial resolution of 100 μm ; (b) Brain maps show exquisite functional detail. For example, the largest increase in cerebral perfusion in our brain mapping study of an auditory challenge (a 1000 Hz/8000 Hz alternating tone) was noted in the caudal portions of auditory cortex [106]. This area has been shown by others using microelectrode tonotopic mapping techniques, to represent sound frequencies in the lower four octaves (from 0.5 to 8 kHz) [109]; (c) Brain maps obtained with the pump demonstrate the functional complexity characteristic of multimodal tasks. Thus, consistent with the complex nature of a locomotor treadmill task, brain activation was demonstrated not only in neural circuits dedicated to motor functions, but also in those engaging sensory and visual functions [107,108]. These results support the

utility of portable infusion pumps as adjunct tools for studying cerebral activation during behavioral challenges in non-tethered, nonrestrained subjects.

5. Mapping brain function during behavioral challenge tests

Brain mapping of behaviors in freely behaving subjects is of interest, not only because it allows access to a set of fundamental behaviors involving extensive motor movement, but also because such activated brain states may serve to accentuate differences that only manifest partially while a subject is in the resting state. In immobilized human subjects, the utility of cognitive ‘stress tests’ to highlight neuronal deficits during functional neuroimaging is well known [110–113]. Similarly, brain mapping performed in ambulatory subjects promises to unmask underlying differences between normal and pathological neural circuits.

In human neuropsychiatric patients such behavioral challenge tests might, for example, include the examination of brain activation during stereotypic movements (e.g. akathisia, tardive dyskinesia, chorea), cataplexy in narcolepsy, compulsions (e.g. hand washing) in obsessive compulsive disorder, or the study of brain activation during motor activity in deficits syndromes such as Parkinson’s disease [114–116]. In addition, more multidimensional behavioral challenges could be studied, such as brain activation during social encounters in subjects with different subtypes of schizophrenia or autism, procedural memory in subtypes of dementia, maternal-infant bonding, or structured versus unstructured play activity in subjects with attention deficit disorder. Some behavioral challenges, such as public speaking in social phobia [117,118], snake exposure in snake phobia [119] or drug craving induced by environmental cues [120–122], though it has been feasible to study these in immobilized subjects, may be more robustly delineated in a natural setting. Furthermore, constraint-free functional neuroimaging may find applications in studying the effects of gender or specific genotypes have on functional brain activation. In addition, functional brain maps obtained at different developmental stages might prove useful in the study of the ontogeny of behavior. This may provide a useful window into understanding childhood mental disorders.

6. Challenges for study design

A critical challenge in functional neuroimaging in freely moving subjects is the definition of the control condition. Brain mapping during complex behaviors requires integration of neural circuits subserving motor, sensory, cognitive and emotional functions. Thus, a control condition for complex behaviors will likely not be represented by a ‘rest as baseline’ condition, but rather by a baseline, which includes a control task. In a standard categorical study design, brain activity during two conditions is compared by subtraction, permitting study of the difference between the full behavioral set and a subset [123]. This requires great attention to the matching of the environmental exposure during the control and test condition, which, given the complexity of the behavior, may in some cases may represent a formidable challenge. Alternatively, one might separate a complex task into several simpler components. The assumption underlying both the subtraction or addition of different conditions in the study of brain activation is that single components of behavior can be

removed or added without interaction. Such an assumption may not always be valid because brain activity and behavior may be characterized by the interaction of their components [124].

In a parametric study design at least two conditions are correlated with a graded behavioral measure, the assumption being that brain activity varies monotonically and systematically with the degree of processing in the dedicated network. Parametric designs, however, typically include more than two test conditions and multiple tracer injections. Hence their application with longer-lived tracers, as is required for functional imaging in freely moving subjects, may become impractical because of accumulating background activity and the possibility with certain tracers of nonhomogeneous washout between the first and second scan.

In a factorial study design, two or more experimental variables (factors) are modulated and the interaction of these factors is assessed. Such an approach has been successfully applied in PET studies that combine both psychological and pharmacological activation. In such studies an interaction of psychological and pharmacological effects on rCBF is taken as evidence of an association between the functional system and neurotransmitter system(s) affected by the drug. For example, attenuation by buspirone (a 5-HT_{1A} receptor partial agonist) of increases in rCBF associated with a word recall task, may represent a direct neuromodulatory effect of this drug, whereas nonspecific effects on rCBF during the control condition may represent a non-modulatory action unrelated to memory [125]. Such an approach may also be usefully applied to functional neuroimaging in freely moving subjects, in which activations noted during specific behavioral challenges are interpreted in the context of their responsiveness to pharmacological intervention.

Having experimental subjects act as their own control, rather than comparing separate control and test groups, allows for a reduction of the intersubject variance. However, additional error may be introduced, including repositioning errors of the subject's head within the scanner, as well as the potential day-to-day biologic variation in baseline states for studies made on 2 different days. While software for three-dimensional realignment may aid in minimizing repositioning errors, detailed reference test-retest studies would be needed to recognize the percentage variation between two studies on the same subject under the same baseline conditions.

In studying cerebral activation in which subjects serve as their own controls, it is frequently useful to utilize a split-dose technique, whereby two doses of the tracer are administered on a single day 1–2 h apart, with the scan following the first administration acting as a control for the scan following the second administration, which is made with the subject in an activated state. The consequences of using tracers with relatively longer half-lives is that, within the time-frame of a typical brain SPECT or PET activation experiment, the second image is substantially contaminated with the remaining activity of the previous injection. In practice, this limits the number of image acquisitions in most activations to two. The possible presence of washout of the tracer between the first and second scan would not be expected to constitute a problem, if such washout occurred homogeneously throughout the brain. In this case, only minor changes would result in the normalized images. However, for

radiotracers in which neuronal washout is not homogeneous, the application of split-dose studies may be limited. This may be the case for ECD [126], though others have disputed this [127]. Here the effect of nonhomogeneous tracer washout could be minimized by spacing out the time between the first and second study by several days [126].

7. Future perspective

In recent years, several groups have demonstrated the application of in vivo neuroreceptor binding techniques to the measurement of acute fluctuations in the concentration of the endogenous transmitters in the vicinity of radio-labeled receptors [128]. This new application of neuroreceptor imaging allows direct measurement of synaptic transmission in specific neurotransmitter systems in the brain, and correlation of these measurements with behaviors and symptoms. In principle, a similar approach might be applicable to the study of dynamic neurotransmission in freely moving subjects.

Imaging of neurotransmitter release has been extensively developed for the study of dopamine transmission at D₂ receptors. The principle underlying this technique is competition between radiotracers and transmitters for binding to neuroreceptors. The original proposition based on a simple occupancy model was that low-affinity radio-tracers bind more 'loosely' to D₂ receptors, and, therefore, are more vulnerable to dopamine competition [129]. Recent work, however, suggests that the affinity of the radiotracer will affect its vulnerability to endogenous dopamine only if dopamine is administered as a pulse, but not if neuro-transmitter levels are maintained constant [128]. Such findings have strong implications for the choice of radio-tracers in potential future applications of the study of dynamic neurotransmission in freely moving subjects. As changes in dopaminergic transmission associated with any acute neurobehavioral challenge are likely to occur with a short onset and offset, affinity of the radiotracer to its receptor will remain a crucial variable. Some authors using simulation studies on the kinetic characteristics of D₂ ligands have suggested that a completely irreversible tracer gives maximum response to a dopamine pulse [130], whereas others have contended that this may be true only if the control and stimulus condition have identical input functions [131]. It is becoming increasingly clear that factors other than changes in neurotransmitter occupancy play a role in the modulation of receptor availability following changes in synaptic neurotransmitter concentration. Clarification of such issues will be necessary before studies of dynamic neurotransmission can be undertaken in freely moving subjects.

The promise of novel experimental approaches outlined above need to be placed in the context of technological and physiological studies which remain to be undertaken to answer some fundamental questions in the field of functional neuroimaging. Although, the existence of a flow/metabolism coupling at rest is well accepted, the exact relationship between neuronal activity, rCBF and metabolism during cerebral activation remains a question of debate. Recent excellent reviews on this topic [132–134] outline a number of pivotal issues that remain to be clarified. These include an improved understanding of (a) why behavioral performance or mental effort shows correlations with rCBF in some, but not other brain regions; (b) the relationship between rCBF measured at the macronetwork level and neuronal activity at the micronetwork level; (c) the role of field potentials compared to

action potentials in altering blood flow changes; (d) the role of excitatory compared to inhibitory neurotransmitters in altering brain perfusion and metabolism; (e) the limits of proxy measures such as rCBF or glucose/oxygen consumption in detecting changes in spatial and temporal neural processing, in which the overall energy demands may remain unchanged; (f) the mechanisms of flow/metabolism uncoupling that have been reported in pathological states or during pharmacological manipulations.

8. Conclusions

Functional neuroimaging in freely moving subjects has been undertaken by a number of investigators in the past using a variety of approaches. Overall, however, it has remained an underutilized approach to studying mammalian behaviors that depend on locomotor activity. Future applications of these methods, as well as the more widespread use of newer radiotracers better suited for constraint-free neuroimaging, promises to increase our understanding of the basic building blocks of normal behavior. Such knowledge may provide the basis of an improved integration of a functional brain anatomy in the context of mental disorders [135].

Acknowledgments

We would like to thank Dr Oscar U. Scremin for his helpful comments regarding this manuscript, and Drs J. Yang, J.R. Bading, and X. Chen for their expert assistance with the ^{64}Cu -PTSM PET data acquisition. Supported by the NIBIB (RO1 EB-00300-03), the Whitaker Foundation (RG-99-0331), and the Veterans Administration.

References

1. Bush M, Custer R, Smeller J, Bush LM. Physiologic measures of nonhuman primates during physical restraint and chemical immobilization. *J Am Vet Med Assoc.* 1977; 171:866–9. [PubMed: 21868]
2. Jacobs B, Chugani HT, Allada V, Chen S, Phelps ME, Pollack DB, Raleigh MJ. Developmental changes in brain metabolism in sedated rhesus macaques and vervet monkeys revealed by positron emission tomography. *Cereb Cortex.* 1995; 5:222–33. [PubMed: 7613078]
3. Ma XM, Levy A, Lightman SL. Emergence of an isolated arginine vasopressin (AVP) response to stress after repeated restraint: a study of both AVP and corticotropin-releasing hormone messenger ribonucleic acid (RNA) and heteronuclear RNA. *Endocrinology.* 1997; 138:4351–7. [PubMed: 9322950]
4. Hauger RL, Lorang M, Irwin M, Aguilera G. CRF receptor regulation and sensitization of ACTH responses to acute ether stress during chronic intermittent immobilization stress. *Brain Res.* 1990; 532:34–40. [PubMed: 2178035]
5. Mizugaki M, Nakagawa N, Nakamura H, Hishinuma T, Tomioka Y, Ishiwata S, Ido T, Iwata R, Funaki Y, Itoh M, Higuchi M, Okamura N, Fujiwara T, Sato M, Shindo K, Yoshida S. Influence of anesthesia on brain distribution of [^{11}C]methamphetamine in monkeys in positron emission tomography (PET) study. *Brain Res.* 2001; 911:173–5. [PubMed: 11511387]
6. Tsukada H, Nishiyama S, Kakiuchi T, Ohba H, Sato K, Harada N, Nakanishi S. Isoflurane anesthesia enhances the inhibitory effects of cocaine and GBR12909 on dopamine transporter: PET studies in combination with microdialysis in the monkey brain. *Brain Res.* 1999; 849:85–96. [PubMed: 10592290]
7. Di Piero V, Ferracuti S, Sabatini U, Tombari D, Di Legge S, Pantano P, Cruccu G, Lenzi GL. Diazepam effects on the cerebral responses to tonic pain: a SPET study. *Psychopharmacology.* 2001; 158:252–8. [PubMed: 11713614]

8. Veselis RA, Reinsel RA, Beattie BJ, Mawlawi OR, Feshchenko VA, DiResta GR, Larson SM, Blasberg RG. Midazolam changes cerebral blood flow in discrete brain regions: an H₂(¹⁵O) positron emission tomography study. *Anesthesiology*. 1997; 87:1106–17. [PubMed: 9366463]
9. Wang GJ, Volkow ND, Overall J, Hitzemann RJ, Pappas N, Pascani K, Fowler JS. Reproducibility of regional brain metabolic responses to lorazepam. *J Nucl Med*. 1996; 37:1609–13. [PubMed: 8862292]
10. Madsen PL, Sperling BK, Warming T, Schmidt JF, Secher NH, Wildschiodtz G, Holm S, Lassen NA. Middle cerebral artery blood velocity and cerebral blood flow and O₂ uptake during dynamic exercise. *J Appl Physiol*. 1993; 74:245–50. [PubMed: 8444699]
11. Globus M, Melamed E, Keren A, Tzivoni D, Granot C, Lavy S, Stern S. Effect of exercise on cerebral circulation. *J Cereb Blood Flow Metab*. 1983; 3:287–90. [PubMed: 6409908]
12. Thomas SN, Schroeder T, Secher NH, Mitchell JH. Cerebral blood flow during submaximal and maximal dynamic exercise in humans. *J Appl Physiol*. 1989; 67:744–8. [PubMed: 2507500]
13. Obayashi S, Suhara T, Kawabe K, Okauchi T, Maeda J, Akine Y, Onoe H, Iriki A. Functional brain mapping of monkey tool use. *Neuroimage*. 2001; 14:853–61. [PubMed: 11554804]
14. Bryan RM Jr. A method for measuring regional cerebral blood flow in freely moving, unstressed rats. *J Neurosci Methods*. 1986; 17:311–22. [PubMed: 3537542]
15. Pannier JL, Leusen I. Regional blood flow in response to exercise in conscious dogs. *Eur J Appl Physiol Occup Physiol*. 1977; 36:255–65. [PubMed: 902639]
16. Gross PM, Marcus ML, Heistad DD. Regional distribution of cerebral blood flow during exercise in dogs. *J Appl Physiol*. 1980; 48:213–7. [PubMed: 6767665]
17. Foreman DL, Sanders M, Bloor CM. Total and regional cerebral blood flow during moderate and severe exercise in miniature swine. *J Appl Physiol*. 1976; 40:191–5. [PubMed: 2577]
18. Delp MD, Armstrong RB, Godfrey DA, Laughlin MH, Ross CD, Wilkerson MKIDMD. Exercise increases blood flow to locomotor, vestibular, cardiorespiratory and visual regions of the brain in miniature swine. *J Physiol*. 2001; 533:849–59. [PubMed: 11410640]
19. Sandor P, Demchenko IT, Morgalyov YN, Moskalenko YE, Kovach AG. Cerebral blood flow and tissue pO₂ changes following local met-enkephalin administration in awake, freely moving cats. *Acta Physiol Hung*. 1983; 61:155–61. [PubMed: 6650185]
20. Fellows LK, Boutelle MG. Rapid changes in extracellular glucose levels and blood flow in the striatum of the freely moving rat. *Brain Res*. 1993; 604:225–31. [PubMed: 8457850]
21. Le Maho Y, Karmann H, Briot D, Handrich Y, Robin JP, Mioskowski E, Cherel Y, Farni J. Stress in birds due to routine handling and a technique to avoid it. *Am J Physiol*. 1992; 263:R775–81. [PubMed: 1415787]
22. Loijens LW, Schouten WG, Wiepkema PR, Wiegant VM. Brain opioid receptor density reflects behavioral and heart rate responses in pigs. *Physiol Behav*. 2002; 76:579–87. [PubMed: 12126996]
23. Redbo I. Relations between oral stereotypies, open-field behavior, and pituitary-adrenal system in growing dairy cattle. *Physiol Behav*. 1998; 64:273–8. [PubMed: 9748093]
24. Schumacher SJ, Morris M, Riddick E. Effects of restraint by tether jackets on behavior in spontaneously hypertensive rats. *Clin Exp Hypertension—Part A, Theory Practice*. 1991; 13:875–84.
25. Vestergaard K, Hansen LL. Tethered versus loose sows: ethological observations and measures of productivity. I. Ethological observations during pregnancy and farrowing. *Ann Rech Vet*. 1984; 15:245–56. [PubMed: 6486696]
26. Becker B, Christenson R, Ford J, Manak R, Nienaber J, Hahn G, Deshazer J. Serum cortisol concentrations in gilts and sows housed in tether stalls, gestation stalls and individual pens. *Ann Rech Vet*. 1984; 15:237–42. [PubMed: 6486695]
27. Kimura A, Okada K, Sato A, Suzuki H. Regional cerebral blood flow in the frontal, parietal and occipital cortices increases independently of systemic arterial pressure during slow walking in conscious rats. *Neurosci Res*. 1994; 20:309–15. [PubMed: 7870384]
28. Helmchen F, Fee MS, Tank DW, Denk W. A miniature head-mounted two-photon microscope high-resolution brain imaging in freely moving animals. *Neuron*. 2001; 31:903–12. [PubMed: 11580892]

29. Oohashi T, Kawai N, Honda M, Nakamura S, Morimoto M, Nishina E, Maekawa T. Electroencephalographic measurement of possession trance in the field. *Clin Neurophysiol.* 2002; 113:435–45. [PubMed: 11897544]
30. Herold N, Spray S, Horn T, Henriksen SJ. Measurements of behavior in the naked mole-rat after intraperitoneal implantation of a radio-telemetry system. *J Neurosci Methods.* 1998; 81:151–8. [PubMed: 9696320]
31. Kling AS, Lloyd RL, Perryman KM. Slow wave changes in amygdala to visual, auditory, and social stimuli following lesions of the inferior temporal cortex in squirrel monkey (*Saimiri sciureus*). *Behav Neural Biol.* 1987; 47:54–72. [PubMed: 3566692]
32. Kling A, Steklis HD, Deutsch S. Radiotelemetered activity from the amygdala during social interactions in the monkey. *Exp Neurol.* 1979; 66:88–96. [PubMed: 113240]
33. Stevens JR, Bigelow L, Denney D, Lipkin J, Livermore AH Jr, Rauscher F, Wyatt RJ. Telemetered EEG-EOG during psychotic behaviors of schizophrenia. *Arch General Psychiatr.* 1979; 36:251–62.
34. Pearce PC, Crofts HS, Muggleton NG, Scott EA. Concurrent monitoring of EEG and performance in the common marmoset: a methodological approach. *Physiol Behav.* 1998; 63:591–9. [PubMed: 9523903]
35. Morgan JI, Curran T. Stimulus-transcription coupling in the nervous system: involvement of the inducible proto-oncogenes fos and jun. *Annu Rev Neurosci.* 1991; 14:421–51. [PubMed: 1903243]
36. Armstrong RC, Montminy MR. Transsynaptic control of gene expression. *Annu Rev Neurosci.* 1993; 16:17–29. [PubMed: 8384807]
37. Rouiller EM, Wan XS, Moret V, Liang F. Mapping of c-fos expression elicited by pure tones stimulation in the auditory pathways of the rat, with emphasis on the cochlear nucleus. *Neurosci Lett.* 1992; 144:19–24. [PubMed: 1436702]
38. Vischer MW, Hausler R, Rouiller EM. Distribution of Fos-like immunoreactivity in the auditory pathway of the Sprague–Dawley rat elicited by cochlear electrical stimulation. *Neurosci Res.* 1994; 19:175–85. [PubMed: 8008246]
39. Wong-Riley MT. Cytochrome oxidase: an endogenous metabolic marker for neuronal activity. *Trends Neurosci.* 1989; 12:94–101. [PubMed: 2469224]
40. Nie F, Wong-Riley MT. Mitochondrial- and nuclear-encoded subunits of cytochrome oxidase in neurons: differences in compartmental distribution, correlation with enzyme activity, and regulation by neuronal activity. *J Comp Neurol.* 1996; 373:139–55. [PubMed: 8876469]
41. Luo XG, Kong XY, Wong-Riley MT. Effect of monocular enucleation or impulse blockage on gamma-aminobutyric acid and cytochrome oxidase levels in neurons of the adult cat lateral geniculate nucleus. *Vis Neurosci.* 1991; 6:55–68. [PubMed: 1851037]
42. de la Torre JC, Cada A, Nelson N, Davis G, Sutherland RJ, Gonzalez-Lima F. Reduced cytochrome oxidase and memory dysfunction after chronic brain ischemia in aged rats. *Neurosci Lett.* 1997; 223:165–8. [PubMed: 9080458]
43. LaManna JC, Kutina-Nelson KL, Hritz MA, Huang Z, Wong-Riley MT. Decreased rat brain cytochrome oxidase activity after prolonged hypoxia. *Brain Res.* 1996; 720:1–6. [PubMed: 8782890]
44. Ferrandiz ML, Martinez M, De Juan E, Diez A, Bustos G, Miquel J. Impairment of mitochondrial oxidative phosphorylation in the brain of aged mice. *Brain Res.* 1994; 644:335–8. [PubMed: 8050045]
45. Nobrega JN, Raymond R, DiStefano L, Burnham WM. Long-term changes in regional brain cytochrome oxidase activity induced by electroconvulsive treatment in rats. *Brain Res.* 1993; 605:1–8. [PubMed: 8385539]
46. Agin V, Chicher R, Chichery MP. Effects of learning on cytochrome oxidase activity in cuttlefish brain. *Neuroreport.* 2001; 12:113–6. [PubMed: 11201069]
47. Poremba A, Jones D, Gonzalez-Lima F. Classical conditioning modifies cytochrome oxidase activity in the auditory system. *Eur J Neurosci.* 1998; 10:3035–43. [PubMed: 9786198]
48. Agin V, Chichery R, Maubert E, Chichery MP. Time-dependent effects of cycloheximide on long-term memory in the cuttlefish. *Pharmacol Biochem Behav.* 2003; 75:141–6. [PubMed: 12759122]

49. McCloskey DP, Adamo DS, Anderson BJ. Exercise increases metabolic capacity in the motor cortex and striatum, but not in the hippocampus. *Brain Res.* 2001; 891:168–75. [PubMed: 11164820]
50. Sokoloff L, Reivich M, Kennedy C, Des Rosiers MH, Patlak CS, Pettigrew KD, Sakurada O, Shinohara M. The [^{14}C]deoxyglucose method for the measurement of local cerebral glucose utilization: theory, procedure, and normal values in the conscious and anesthetized albino rat. *J Neurochem.* 1977; 28:897–916. [PubMed: 864466]
51. Lear JL, Ackerlmann RF. Comparison of cerebral glucose metabolic rates measured with fluorodeoxyglucose and glucose labeled in the 1, 2, 3, 4, and 6 positions using double label quantitative digital autoradiography. *J Cereb Blood Flow Metab.* 1988; 8:575–85. [PubMed: 3392117]
52. Ishii K, Senda M, Toyama M, Oda K, Ishii S, Ishiwata K, Sasaki T, Bando M. Brain function associated with bipedal gait—a PET study. *J Cereb Blood Flow Metab.* 1993; 13(Suppl 1):S521.
53. Mishina M, Senda M, Ishii K, Ohshima M, Kitamura S, Katayama Y. Cerebellar activation during ataxic gait in olivopontocerebellar atrophy: a PET study. *Acta Neurol Scand.* 1999; 100:369–76. [PubMed: 10589796]
54. Blaizot X, Landeau B, Baron JC, Chavoix C. Mapping the visual recognition memory network with PET in the behaving baboon. *J Cereb Blood Flow Metab.* 2000; 20:213–9. [PubMed: 10698057]
55. Prins ML, Hovda DA. Mapping cerebral glucose metabolism during spatial learning: interactions of development and traumatic brain injury. *J Neurotrauma.* 2001; 18:31–46. [PubMed: 11200248]
56. Gonzalez-Lima F, Helmstetter FJ, Agudo J. Functional mapping of the rat brain during drinking behavior: a fluorodeoxyglucose study. *Physiol Behav.* 1993; 54:605–12. [PubMed: 8415957]
57. Greenough W. Structural correlates of information storage in the mammalian brain: a review and hypothesis. *Trends Neurosci.* 1984; 7:229–33.
58. Schwartzman RJ, Eidelberg E, Alexander GM. Asymmetrical regional changes in energy metabolism of the central nervous system during walking. *Brain Res.* 1986; 398:113–20. [PubMed: 3801884]
59. Weissman AD, Marquis KL, Moreton JE, London ED. Effects of self-administered phencyclidine on regional uptake of 2-deoxy-D-1- ^{14}C]glucose in brain. *Neuropharmacology.* 1989; 28:575–83. [PubMed: 2755563]
60. Pontieri FE, Crane AM, Seiden LS, Kleven MS, Porrino LJ. Metabolic mapping of the effects of intravenous methamphetamine administration in freely moving rats. *Psychopharmacology.* 1990; 102:175–82. [PubMed: 1980372]
61. Ligeti L, Hines K, Dora E, Sinnwell T, Huang MT, McLaughlin AC. Cerebral blood flow and metabolic rate in the conscious, freely moving rat: the effects of hypercapnia, and acute ethanol administration. *Alcohol Clin Exp Res.* 1991; 15:766–70. [PubMed: 1755506]
62. Jay TM, Jouvet M, des Rosiers MH. Local cerebral glucose utilization in the free moving mouse: a comparison during two stages of the activity-rest cycle. *Brain Res.* 1985; 342:297–306. [PubMed: 4041831]
63. Mori K, Schmidt K, Jay T, Palombo E, Nelson T, Lucignani G, Pettigrew K, Kennedy C, Sokoloff L. Optimal duration of experimental period in measurement of local cerebral glucose utilization with the deoxyglucose method. *J Neurochem.* 1990; 54:307–19. [PubMed: 2403433]
64. Phelps ME, Huang SC, Hoffman EJ, Selin C, Kuhl DE. Cerebral extraction of N-13 ammonia: its dependence on cerebral blood flow and capillary permeability—surface area product. *Stroke.* 1981; 12:607–19. [PubMed: 7303045]
65. Maziere B, Loc'h C, Steinling M, Comar D. Stable labelling of serum albumin microspheres with gallium-68. *Int J Rad Appl Instrum [A].* 1986; 37:360–1.
66. Steinling M, Baron JC, Maziere B, Lasjaunias P, Loc'h C, Cabanis EA, Guillon B. Tomographic measurement of cerebral blood flow by the ^{68}Ga -labelled-microsphere and continuous- C^{15}O_2 -inhalation methods. *Eur J Nucl Med.* 1985; 11:29–32. [PubMed: 3930249]
67. Fukuyama H, Ouchi Y, Matsuzaki S, Nagahama Y, Yamauchi H, Ogawa M, Kimura J, Shibasaki H. Brain functional activity during gait in normal subjects: a SPECT study. *Neurosci Lett.* 1997; 228:183–6. [PubMed: 9218638]

68. Williamson JW, Nobrega AC, McColl R, Mathews D, Winchester P, Friberg L, Mitchell JH. Activation of the insular cortex during dynamic exercise in humans. *J Physiol.* 1997; 503:277–83. [PubMed: 9306272]
69. Catafau AM, Parellada E, Lomena F, Bernardo M, Setoain J, Catarineu S, Pavia J, Herranz R, Gonzalez-Monclus E, Lomena FJ, Ros D. Role of the cingulate gyrus during the Wisconsin Card Sorting Test: a single photon emission computed tomography study in normal volunteers. *Psychiatr Res.* 1998; 83:67–74.
70. Neirinckx RD, Canning LR, Piper IM, Nowotnik DP, Pickett RD, Holmes RA, Volkert WA, Forster AM, Weisner PS, Marriott JA, et al. Technetium-99m D,L-HM-PAO: a new radiopharmaceutical for SPECT imaging of regional cerebral blood perfusion. *J Nucl Med.* 1987; 28:191–202. [PubMed: 3492596]
71. Andersen AR, Friberg HH, Schmidt JF, Hasselbalch SG. Quantitative measurements of cerebral blood flow using SPECT and [^{99m}Tc]-D,L-HM-PAO compared to Xenon-133. *J Cereb Blood Flow Metab.* 1988; 8:S69–81. [PubMed: 3263980]
72. Yonekura Y, Nishizawa S, Mukai T, Fujita T, Fukuyama H, Ishikawa M, Kikuchi H, Konishi J, Andersen AR, Lassen NA. SPECT with [^{99m}Tc]-D,L-hexamethyl-propylene amine oxime (HM-PAO) compared with regional cerebral blood flow measured by PET: effects of linearization. *J Cereb Blood Flow Metab.* 1988; 8:S82–9. [PubMed: 3263981]
73. Creutzig H, Schober O, Gielow P, Friedrich R, Becker H, Dietz H, Hundeshagen H. Cerebral dynamics of *N*-isopropyl-(¹²³I)*p*-iodoamphetamine. *J Nucl Med.* 1986; 27:178–83. [PubMed: 3486950]
74. Raynaud C, Rancurel G, Samson Y, Baron JC, Soucy JP, Kieffer E, Cabanis E, Majdalani A, Ricard S, Bardy A, et al. Pathophysiologic study of chronic infarcts with I-123 isopropyl iodoamphetamine (IMP): the importance of periinfarct area. *Stroke.* 1987; 18:21–9. [PubMed: 3492789]
75. Yonekura Y, Nishizawa S, Mukai T, Iwasaki Y, Fukuyama H, Ishikawa M, Tamaki N, Konishil J. Functional mapping of flow and back-diffusion rate of *N*-isopropyl-*p*-iodoamphetamine in human brain. *J Nucl Med.* 1993; 34:839–44. [PubMed: 8478721]
76. Buell U, Krappel W, Schmiedek P, et al. I-123 amphetamine vs Xe-133 SPECT. A comparative study in patients with unilateral cerebrovascular disease (CVD) (Abstract). *J Nucl Med.* 1985; 26:P25.
77. Barthel H, Kampfer I, Seese A, Dannenberg C, Kluge R, Burchert W, Knapp WH. Improvement of brain SPECT by stabilization of Tc-99m-HMPAO with methylene blue or cobalt chloride. Comparison with Tc-99m-ECD. *Nuklearmedizin.* 1999; 38:80–4. [PubMed: 10320993]
78. Goethals I, Audenaert K, Jacobs F, Van De Wiele C, Vermeir G, Vandierendonck A, Van Heeringen C, Dierckx R. Toward clinical application of neuropsychological activation probes with SPECT: a spatial working memory task. *J Nucl Med.* 2002; 43:1426–31. [PubMed: 12411543]
79. Audenaert K, Brans B, Van Laere K, Lahorte P, Versijpt J, van Heeringen K, Dierckx R. Verbal fluency as a prefrontal activation probe: a validation study using ^{99m}Tc-ECD brain SPET. *Eur J Nucl Med.* 2000; 27:1800–8. [PubMed: 11189943]
80. Audenaert K, Lahorte P, Brans B, van Laere K, Goethals I, van Heeringen K, Dierckx RA. The classical stroop interference task as a prefrontal activation probe: a validation study using ^{99m}Tc-ECD brain SPECT. *Nucl Med Commun.* 2001; 22:135–43. [PubMed: 11258399]
81. Walovitch RC, Cheesman EH, Maheu LJ, Hall KM. Studies of the retention mechanism of the brain perfusion imaging agent ^{99m}Tc-bicisate (^{99m}Tc-ECD). *J Cereb Blood Flow Metab.* 1994; 14(Suppl 1):S4–11. [PubMed: 8263070]
82. Leveille J, Demonceau G, De Roo M, Rigo P, Taillefer R, Morgan RA, Kupranick D, Walovitch RC. Characterization of technetium-99m-L,L-ECD for brain perfusion imaging, part 2: biodistribution and brain imaging in humans. *J Nucl Med.* 1989; 30:1902–10. [PubMed: 2809757]
83. Walovitch RC, Hill TC, Garrity ST, Cheesman EH, Burgess BA, O'Leary DH, Watson AD, Ganey MV, Morgan RA, Williams SJ. Characterization of technetium-99m-L,L-ECD for brain perfusion imaging, part 1: pharmacology of technetium-99m ECD in nonhuman primates. *J Nucl Med.* 1989; 30:1892–901. [PubMed: 2809756]

84. Koyama M, Kawashima R, Ito H, Ono S, Sato K, Goto R, Kinomura S, Yoshioka S, Sato T, Fukuda H. SPECT imaging of normal subjects with technetium-99m-HMPAO and technetium-99m-ECD. *J Nucl Med.* 1997; 38:587–92. [PubMed: 9098207]
85. Leveille J, Demonceau G, Walovitch RC. Intrasubject comparison between technetium-99m-ECD and technetium-99m-HMPAO in healthy human subjects. *J Nucl Med.* 1992; 33:480–4. [PubMed: 1552328]
86. Catafau AM. Brain SPECT in clinical practice. Part I: perfusion. *J Nucl Med.* 2001; 42:259–71. [PubMed: 11216525]
87. Lassen NA, Andersen AR, Friberg L, Paulson OB. The retention of [^{99m}Tc]-D,L-HM-PAO in the human brain after intracarotid bolus injection: a kinetic analysis. *J Cereb Blood Flow Metab.* 1988; 8:S13–22. [PubMed: 3192638]
88. Friberg L, Andersen AR, Lassen NA, Holm S, Dam M. Retention of ^{99m}Tc-bicisate in the human brain after intracarotid injection. *J Cereb Blood Flow Metab.* 1994; 14(Suppl 1):S19–27. [PubMed: 8263067]
89. Devous MD, Payne JK Sr, Lowe JL, Leroy RF. Comparison of technetium-99m-ECD to Xenon-133 SPECT in normal controls and in patients with mild to moderate regional cerebral blood flow abnormalities. *J Nucl Med.* 1993; 34:754–61. [PubMed: 8478707]
90. Tsuchida T, Nishizawa S, Yonekura Y, Sadato N, Iwasaki Y, Fujita T, Matoba N, Magata Y, Tamaki N, Konishi J. SPECT images of technetium-99m-ethyl cysteinyl dimer in cerebrovascular diseases: comparison with other cerebral perfusion tracers and PET. *J Nucl Med.* 1994; 35:27–31. [PubMed: 8271056]
91. Inoue Y, Abe O, Kawakami T, Ozaki T, Inoue M, Yokoyama I, Yoshikawa K, Ohtomo K. Metabolism of ^{99m}Tc-ethylcysteinyl dimer in infarcted brain tissue of rats. *J Nucl Med.* 2001; 42:802–7. [PubMed: 11337580]
92. Mathias CJ, Welch MJ, Raichle ME, Mintun MA, Lich LL, McGuire AH, Zinn KR, John EK, Green MA. Evaluation of a potential generator-produced PET tracer for cerebral perfusion imaging: single-pass cerebral extraction measurements and imaging with radiolabeled Cu-PTSM. *J Nucl Med.* 1990; 31:351–9. [PubMed: 2308007]
93. McCarthy DW, Bass LA, Cutler PD, Shefer RE, Klinkowstein RE, Herrero P, Lewis JS, Cutler CS, Anderson CJ, Welch MJ. High purity production and potential applications of copper-60 and copper-61. *Nucl Med Biol.* 1999; 26:351–8. [PubMed: 10382836]
94. Di Rocco RJ, Silva DA, Kuczynski BL, Narra RK, Ramalingam K, Jurisson S, Nunn AD, Eckelman WC. The single-pass cerebral extraction and capillary permeability-surface area product of several putative cerebral blood flow imaging agents. *J Nucl Med.* 1993; 34:641–8. [PubMed: 8455082]
95. Green MA, Klippenstein DL, Tennison JR. Copper(II) bis(thiosemicarbazone) complexes as potential tracers for evaluation of cerebral and myocardial blood flow with PET. *J Nucl Med.* 1988; 29:1549–57. [PubMed: 3261785]
96. Okazawa H, Yonekura Y, Fujibayashi Y, Nishizawa S, Magata Y, Ishizu K, Tanaka F, Tsuchida T, Tamaki N, Konishi J. Clinical application and quantitative evaluation of generator-produced copper-62-PTSM as a brain perfusion tracer for PET. *J Nucl Med.* 1994; 35:1910–5. [PubMed: 7989968]
97. Green MA, Mathias CJ, Welch MJ, McGuire AH, Perry D, Fernandez-Rubio F, Perlmutter JS, Raichle ME, Bergmann SR. Copper-62-labeled pyruvaldehyde bis(N⁴-methylthiosemicarbazone)copper(II): synthesis and evaluation as a positron emission tomography tracer for cerebral and myocardial perfusion. *J Nucl Med.* 1990; 31:1989–96. [PubMed: 2266398]
98. Wallhaus TR, Lacy J, Whang J, Green MA, Nickles RJ, Stone CK. Human biodistribution and dosimetry of the PET perfusion agent copper-62-PTSM. *J Nucl Med.* 1998; 39:1958–64. [PubMed: 9829589]
99. Mathias CJ, Welch MJ, Lich L, Raichle ME, Volkert WA, Hung JC. Single-pass extraction of D,L and meso Tc-99m HM-PAO in primate brain. *J Nucl Med.* 1988; 21:747–8. (abstract).
100. Blower PJ, Lewis JS, Zweit J. Copper radionuclides and radio-pharmaceuticals in nuclear medicine. *Nucl Med Biol.* 1996; 23:957–80. [PubMed: 9004284]

101. Mathias CJ, Bergmann SR, Green MA. Species-dependent binding of copper(II) bis(thiosemicarbazone) radiopharmaceuticals to serum albumin. *J Nucl Med.* 1995; 36:1451–5. [PubMed: 7629593]
102. Okazawa H, Yonekura Y, Fujibayashi Y, Mukai T, Nishizawa S, Magata Y, Ishizu K, Tamaki N, Konishi J. Measurement of regional cerebral blood flow with copper-62-PTSM and a three-compartment model. *J Nucl Med.* 1996; 37:1089–93. [PubMed: 8965175]
103. Martinez ZA, Colgan M, Baxter LR Jr, Quintana J, Siegel S, Chatziioannou A, Cherry SR, Mazziotta JC, Phelps ME. Oral ¹⁸F-fluoro-2-deoxyglucose for primate PET studies without behavioral restraint: demonstration of principle. *Am J Primatol.* 1997; 42:215–24. [PubMed: 9209586]
104. For a comparative chart of insulin pump rates see www.diabetesnet.com/diabetes_technology/insulin_pump_models.php
105. Holschneider DP, Maarek J-M, Harimoto J, Yang J, Scremin OU. An implantable bolus infusion pump for use in freely moving, non-tethered rats. *Am J Physiol Heart Circ Physiol.* 2002; 283:H1713–9. [PubMed: 12234827]
106. Holschneider DP, Maarek JM, Yang J, Harimoto J, Scremin OU. Activation of cerebral cortex during acoustic challenge or acute foot-shock in freely moving, nontethered rats. *Neurosci Lett.* 2004; 354:74–8. [PubMed: 14698485]
107. Nguyen PT, Holschneider DP, Maarek JM-I, Yang J, Mandelkern MA. Statistical parametric mapping applied to an autoradiographic study of cerebral activation during treadmill walking in rats. *Neuroimage.* 2004 (in press).
108. Holschneider DP, Maarek JM, Yang J, Harimoto J, Scremin OU. Functional brain mapping in freely moving rats during treadmill walking. *J Cerebr Blood Flow Metab.* 2003; 23:925–32.
109. Doron NN, Ledoux JE, Semple MN. Redefining the tonotopic core of rat auditory cortex: physiological evidence for a posterior field. *J Comp Neurol.* 2002; 453:345–60. [PubMed: 12389207]
110. Rauch SL, van der Kolk BA, Fisler RE, Alpert NM, Orr SP, Savage CR, Fischman AJ, Jenike MA, Pitman RK. A symptom provocation study of posttraumatic stress disorder using positron emission tomography and script-driven imagery. *Arch Gen Psychiatr.* 1996; 53:380–7. [PubMed: 8624181]
111. Bremner JD, Staib LH, Kaloupek D, Southwick SM, Soufer R, Charney DS. Neural correlates of exposure to traumatic pictures and sound in Vietnam combat veterans with and without posttraumatic stress disorder: a positron emission tomography study. *Biol Psychiatr.* 1999; 45:806–16.
112. Saykin AJ, Flashman LA, Frutiger SA, Johnson SC, Mamourian AC, Moritz CH, O’Jile JR, Riordan HJ, Santulli RB, Smith CA, Weaver JB. Neuroanatomic substrates of semantic memory impairment in Alzheimer’s disease: patterns of functional MRI activation. *J Intl Neuropsychol Soc.* 1999; 5:377–92.
113. Grady CL, Haxby JV, Horwitz B, Gillette J, Salerno JA, Gonzalez-Aviles A, Carson RE, Herscovitch P, Schapiro MB, Rapoport SI. Activation of cerebral blood flow during a visuo-perceptual task in patients with Alzheimer-type dementia. *Neurobiol Aging.* 1993; 14:35–44. [PubMed: 8450930]
114. Playford ED, Jenkins IH, Passingham RE, Nutt J, Frackowiak RS, Brooks DJ. Impaired mesial frontal and putamen activation in Parkinson’s disease: a positron emission tomography study. *Ann Neurol.* 1992; 32:151–61. [PubMed: 1510355]
115. Jahanshahi M, Jenkins IH, Brown RG, Marsden CD, Passingham RE, Brooks DJ. Self-initiated versus externally triggered movements. I. An investigation using measurement of regional cerebral blood flow with PET and movement-related potentials in normal and Parkinson’s disease subjects. *Brain.* 1995; 118(Pt 4):913–33. [PubMed: 7655888]
116. Jenkins IH, Fernandez W, Playford ED, Lees AJ, Frackowiak RS, Passingham RE, Brooks DJ. Impaired activation of the supplementary motor area in Parkinson’s disease is reversed when akinesia is treated with apomorphine. *Ann Neurol.* 1992; 32:749–57. [PubMed: 1471865]
117. Tillfors M, Furmark T, Marteinsdottir I, Fredrikson M. Cerebral blood flow during anticipation of public speaking in social phobia: a PET study. *Biol Psychiatr.* 2002; 52:1113–9.

118. Tillfors M, Furmark T, Marteinsdottir I, Fischer H, Pissiota A, Langstrom B, Fredrikson M. Cerebral blood flow in subjects with social phobia during stressful speaking tasks: a PET study. *Am J Psychiatr*. 2001; 158:1220–6. [PubMed: 11481154]
119. Fredrikson M, Wik G, Greitz T, Eriksson L, Stone-Elander S, Ericson K, Sedvall G. Regional cerebral blood flow during experimental phobic fear. *Psychophysiology*. 1993; 30:126–30. [PubMed: 8416057]
120. Brody AL, Mandelkern MA, London ED, Childress AR, Lee GS, Bota RG, Ho ML, Saxena S, Baxter LR Jr, Madsen D, Jarvik ME. Brain metabolic changes during cigarette craving. *Arch Gen Psychiatr*. 2002; 59:1162–72. [PubMed: 12470133]
121. Dalgligh MR, Weinstein A, Malizia AL, Wilson S, Melichar JK, Britten S, Brewer C, Lingford-Hughes A, Myles JS, Grasby P, Nutt DJ. Changes in regional cerebral blood flow elicited by craving memories in abstinent opiate-dependent subjects. *Am J Psychiatr*. 2001; 158:1680–6. [PubMed: 11579002]
122. Kilts CD, Schweitzer JB, Quinn CK, Gross RE, Faber TL, Muhammad F, Ely TD, Hoffman JM, Drexler KP. Neural activity related to drug craving in cocaine addiction. *Arch Gen Psychiatr*. 2001; 58:334–41. [PubMed: 11296093]
123. Petersen SE, Fox PT, Posner MI, Mintun M, Raichle ME, Friston KJ, Grasby PM, Frith CD, Bench CJ, Dolan RJ, Cowen PJ, Liddle PF, Frackowiak RS, Price CJ, Fletcher P, Moore C. Positron emission tomographic studies of the cortical anatomy of single-word processing. *Nature*. 1988; 331:585–9. [PubMed: 3277066]
124. Friston KJ, Price CJ, Fletcher P, Moore C, Frackowiak RS, Dolan RJ. The trouble with cognitive subtraction. *Neuroimage*. 1996; 4:97–104. [PubMed: 9345501]
125. Friston KJ, Grasby PM, Frith CD, Bench CJ, Dolan RJ, Cowen PJ, Liddle PF, Frackowiak RS, Price CJ, Fletcher P, Moore C. The neurotransmitter basis of cognition: psychopharmacological activation studies using positron emission tomography. *Ciba Found Symp*. 1991; 163:76–87. [PubMed: 1687731]
126. Holm S, Madsen PL, Sperling B, Lassen NA. Use of ^{99m}Tc -bicisate in activation studies by split-dose technique. *J Cereb Blood Flow Metab*. 1994; 14(Suppl 1):S115–20. [PubMed: 8263065]
127. Yonekura Y, Ishizu K, Okazawa H, Tanaka F, Hattori N, Sadato N, Tsuchida T, Nishizawa S, Tamaki N, Nagamine T, Konishi J, Shibasaki H. Simplified quantification of regional cerebral blood flow with ^{99m}Tc -ECD SPECT and continuous arterial blood sampling. *Ann Nucl Med*. 1996; 10:173–80.
128. Laruelle M. Imaging synaptic neurotransmission with in vivo binding competition techniques: a critical review. *J Cereb Blood Flow Metab*. 2000; 20:423–51. [PubMed: 10724107]
129. Seeman P, Guan HC, Niznik HB. Endogenous dopamine lowers the dopamine D_2 receptor density as measured by [^3H]raclopride: implications for positron emission tomography of the human brain. *Synapse*. 1989; 3:96–7. [PubMed: 2521961]
130. Morris ED, Fisher RE, Alpert NM, Rauch SL. In vivo imaging of neuromodulation using positron emission tomography-optimal ligand characteristics and task length for detection of activation. *Hum Brain Mapp*. 1995; 3:35–55.
131. Endres CJ, Carson RE. Assessment of dynamic neurotransmitter changes with bolus or infusion delivery of neuroreceptor ligands. *J Cereb Blood Flow Metab*. 1998; 18:1196–210. [PubMed: 9809509]
132. Gsell W, De Sadeleer C, Marchalant Y, MacKenzie ET, Schumann P, Dauphin F. The use of cerebral blood flow as an index of neuronal activity in functional neuroimaging: experimental and pathophysiological considerations. *J Chem Neuroanat*. 2000; 20:215–24. [PubMed: 11207420]
133. Keri S, Gulyas B. Four facets of a single brain: behaviour, cerebral blood flow/metabolism, neuronal activity and neurotransmitter dynamics. *Neuroreport*. 2003; 14:1097–106. [PubMed: 12821790]
134. Mintun MA, Lundstrom BN, Snyder AZ, Vlassenko AG, Shulman GL, Raichle ME. Blood flow and oxygen delivery to human brain during functional activity: theoretical modeling and experimental data. *Proc Natl Acad Sci USA*. 2001; 98:6859–64. [PubMed: 11381119]

135. Sharma T, Sheringham J. Brain imaging in psychiatry: what has it done for the patient? *Hosp Med.* 2002; 63:326–7. [PubMed: 12096659]
136. Chatziioannou A, Qi J, Moore A, Annala A, Nguyen K, Leahy R, Cherry SR. Comparison of 3D maximum a posteriori and filtered backprojection algorithms for high-resolution animal imaging with microPET. *IEEE Trans Med Imag.* 2000; 19:507–12.
137. Qi J, Leahy RM, Cherry SR, Chatziioannou A, Farquhar TH. High-resolution 3D Bayesian image reconstruction using the microPET small-animal scanner. *Phys Med Biol.* 1998; 43:1001–13. [PubMed: 9572523]

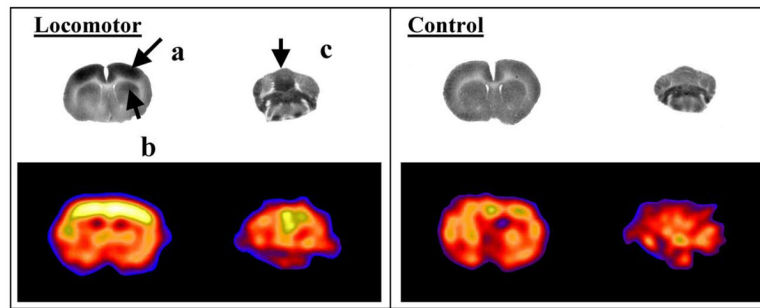


Fig. 1.

Changes in cerebral blood flow-related tissue radioactivity elicited during treadmill walking in the rat compared to a quiescent control. In the locomotor paradigm, the tracer was injected while the rat was walking for 5 min on a RotaRod treadmill. Injection during the control condition occurred while the animal was resting quietly in a transport cage placed next to the RotaRod. Row 1: Coronal autoradiographs of the distribution of [^{14}C]-iodoantipyrine tissue radioactivity show activation of (a) primary motor cortex, (b) dorsolateral striatum, as well as (c) midline cerebellum in the exercising animal [108]. Row 2: Coronal section in a rat obtained using a micro-PET R4 Rodent scanner (Concorde Microsystems, Inc., Knoxville, TN) after administration of [^{64}Cu]-PTSM (1.25 mCi/kg), show a similar activation pattern to that obtained with [^{14}C]-iodoantipyrine. Increased CBF tissue radioactivity is depicted in warmer colors. Brightness was normalized between the two rat PET studies based on a defined region within the piriform cortex, which did not display any significant change in response to the treadmill paradigm. Enhanced resolution of the PET images was obtained using maximum-a-posteriori (MAP) reconstruction [136,137].